

Machine learning enabled the design of compact and efficient wavelength demultiplexing photonic devices

M. Turduev¹, E. Bor², O. Alparslan³, Y. S. Hanay⁴, H. Kurt⁵, S. Arakawa³, and M. Murata³

1. Department of Electrical and Electronics Engineering, Kyrgyz Turkish Manas University, Bishkek 720042, Kyrgyzstan
2. Department of Electrical and Electronics Engineering, TOBB University of Economics and Technology, Ankara 06560, Turkey
3. Graduate School of Information Science and Technology, Osaka University, Osaka 565-0871, Japan
4. Department of Computer Engineering, Akdeniz University, Antalya 07070, Turkey
5. School of Electrical Engineering, Korea Advanced Institute of Science and Technology, Daejeon, 34141, Republic of Korea
mirbek.turduev@manas.edu.kg

Abstract— In this paper, we introduce the design approach of integrated photonic devices by employing reinforcement learning known as attractor selection (AttSel). Here, we combined 3D FDTD with AttSel algorithm, which is based on artificial neural networks, to achieve ultra-compact and highly efficient wavelength demultiplexers with low crosstalk such as. The presented devices consist of SOI materials, which are compatible with complementary MOS technology. Consequently, the reinforcement learning is successfully applied to design smaller and superior integrated photonic devices.

Keywords—wavelength demultiplexing, inverse design, machine learning

I. INTRODUCTION

Traditional photonic device design relies on intuition and manual adjustment of a few parameters, limiting efficiency. However, innovative approaches integrating optimization algorithms and numerical methods have revolutionized the field, enabling accurate calculations of light-matter interactions [1-3]. Recently, "inverse-design" methods using silicon-on-insulator (SOI) materials have emerged, allowing for the design of ultra-compact, highly efficient, CMOS-compatible integrated photonic devices. Convex optimization is employed for wavelength demultiplexer design [4, 5]. Recent developments in machine learning and artificial neural networks have fueled interest among researchers in the design of photonic metasurfaces and Bragg grating devices [6,7]. Furthermore, reinforcement learning techniques have been utilized to design optical couplers and asymmetric light transmitters [8, 9].

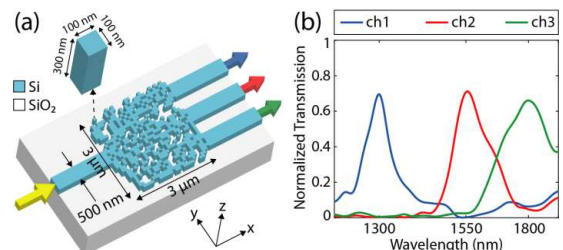


Fig. 1. (a) Perspective view of designed device for demultiplexing the wavelengths of 1300 nm, 1550 nm, 1800 nm) with its structural parameters and (b) plots of normalized transmission efficiencies at the output waveguides. Same colors are used for arrays at output waveguides and corresponding calculated transmission efficiencies.

In this study, we showcase the design of near-infrared wavelength demultiplexers (WDM) using the attractor selection (AttSel) algorithm. AttSel is a reinforcement learning approach based on artificial neural networks [9]. The designed structures achieve exceptional optical performance within a remarkably compact footprint. Detailed numerical investigations of these structures are provided.

II. DESIGN APPROACH AND NUMERICAL INVESTIGATION OF INTEGRATED PHOTONIC DEVICES

AttSel models the interaction of the metabolic reaction network and the gene regulatory network in a cell [10]. Cell growth depends on converting environmental nutrition through metabolic protein reactions. Gene expression levels control protein production, which adjusts based on substance production rates. Favorable conditions create stable attractor states, while unfavorable conditions prompt the cell to search for new expression levels. Noise-induced deviations drive

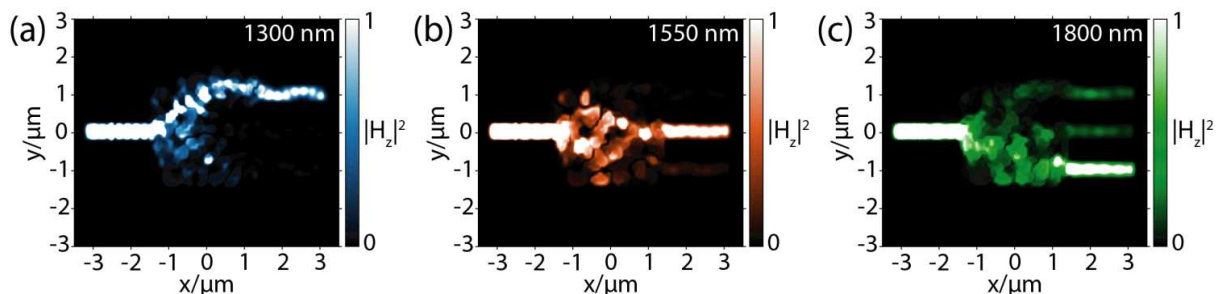


Fig. 2. Calculated magnetic field intensity distributions at the wavelengths of (a) 1300 nm, (b) 1550 nm and (c) 1800 nm for the firstly designed wavelengths demultiplexer device.

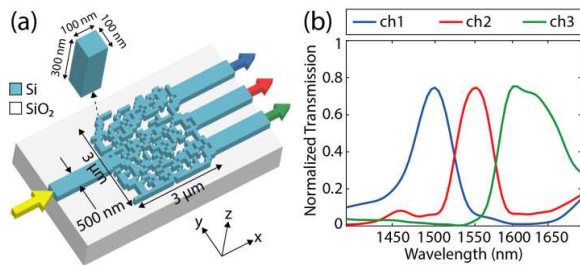


Fig. 3. (a) Perspective view of designed device for demultiplexing the wavelengths of 1500 nm, 1550 nm, 1600 nm) with its structural parameters and (b) plots of normalized transmission efficiencies at the output waveguides. Same colors are used for arrays at output waveguides and corresponding calculated transmission efficiencies.

exploration until favorable conditions are restored. The individual cells in the photonic device can be interpreted as the proteins, whose expression levels are represented as $x = (x_1, x_2, \dots, x_n)$. If the expression level of x_i , which is between $[-1, 1]$, is $x_i < 0$, then the i^{th} individual cell in the photonic device is defined to be an air. Otherwise, it is defined to be Si.

In this study, by applying AttSel, we designed photonic structures with sizes of $3 \times 3 \mu\text{m}^2$ and slab thickness of 300 nm which are composed of Si material on a SiO_2 substrate. The design area is divided into square pixels with dimensions of $100 \times 100 \text{ nm}^2$ where the algorithm determined the states of each pixel to be Si or air according to the desired optical property. Here, the refractive indices of Si and air are fixed as $n_{\text{Si}}=3.46$ and $n_{\text{air}}=1.0$, respectively, at near-infrared wavelengths around 1550 nm. Input and output waveguides having width of 500 nm are connected to design area to form a photonic device.

Here, we present the WDM which separates the incident wavelengths of 1300 nm, 1550 nm and 1800 nm to different output waveguides. Guided-mode TE_0 is considered as incident light in 3D FDTD simulations. The algorithm increases the transmission efficiency of a desired wavelength in a selected waveguide. The corresponding photonic device is represented in Figure 1(a). The distance between adjacent output waveguides is 500 nm. The transmission efficiencies are calculated as 70% (-1.55 dB), 71% (-1.48 dB) and 66% (-1.80 dB) at the selected wavelengths of 1300 nm, 1550 nm and 1800 nm, respectively, see Fig. 1(b). Here, there exist negligible level of crosstalk which is under -12 dB and points out efficient demultiplexing. In Fig. 2, magnetic field intensity ($|H_z|^2$) distributions are presented at selected wavelengths. Here, the incident light at wavelength of 1300 nm is directed to the upper

output waveguide whereas wavelength of 1800 nm is canalized to lower output waveguide. The middle output waveguide conducts the wavelengths at around 1550 nm.

In WDM systems, compactness, channel spacing, number of channels, high transmission efficiency and low crosstalk are highly desirable criteria. For this reason, AttSel is applied to fulfil all the requirements in a WDM device. Here, we designed another photonic device to separate closely selected wavelengths of 1500 nm, 1550 nm and 1600 nm with transmission efficiencies of 75% (-1.25 dB) at different output waveguides. The designed photonic devices are schematically represented in Figure 3(a) with its structural parameters. Also, the corresponding transmission efficiencies are plotted in Figure 3(b). In addition, we extracted the magnetic field distributions at the selected wavelengths which are presented in Figure 4. It is clear to see that the proposed device is capable of demultiplexing the selected wavelengths with small channel spacing of 50 nm. The proposed wavelength demultiplexer can separate three wavelengths between 1500 nm and 1600 nm with channel spacing of 50 nm. Also, our device has ultra-compact sizes of $9.0 \mu\text{m}^2$ and transmission efficiencies -1.25 dB . Proposed structure ultra-compact footprint and high transmission efficiencies for a slightly larger channel spacing of 10 nm. Also, it has low crosstalk between waveguides even if the waveguides are closely placed to each other with 500 nm.

REFERENCES

- [1] Bor E, Turdnev M and Kurt H 2016 *Sci. Rep.* **6** 30781
- [2] Turdnev M, Bor E and Kurt H 2017 *J. Phys. D* **50** 38LT02
- [3] Bor E, Turdnev M and Kurt H 2019 *J. Opt.* **21** 085801
- [4] Piggott A Y, Lu J, Lagoudakis K G, Petykiewicz J, Babinec T M and Vuckovic J 2015 *Nat. Photonics* **9** 374
- [5] Su L, Piggott A Y, Sapra N V, Petykiewicz J and Vuckovic J 2017 *ACS Photonics* **5** 301
- [6] Nadell C C, Huang B, Malof J M and Padilla W J 2019 *Opt. Express* **27** 27523.
- [7] Gao L, Li X, Liu D, Wang L and Yu Z 2019 *Adv. Mater.* **31** 1905467
- [8] Turdnev M, Bor E, Latifoglu C, Giden I H, Hanay Y S and Kurt H 2018 *J. Lightwave Technol.* **36** 2812
- [9] Bor E, Alparslan O, Turdnev M, Hanay Y S, Kurt H, Arakawa S and Murata M 2018 *Opt. Express* **26** 29032
- [10] Kashiwagi A, Urabe I, Kaneko K and Yomo T 2006 *PLoS One* **1** e49.

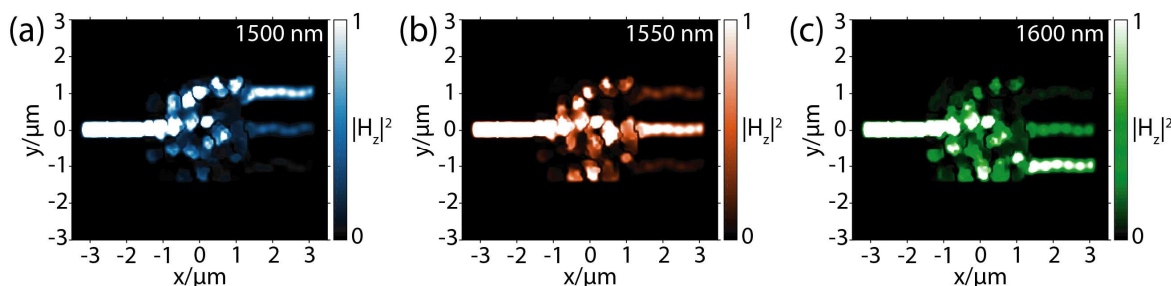


Fig. 4. Calculated magnetic field intensity distributions at the wavelengths of (a) 1500 nm, (b) 1550 nm and (c) 1600 nm for the secondly designed wavelengths demultiplexer device.